Food Chemistry 305 (2020) 125463

Contents lists available at ScienceDirect

Food Chemistry

journal homepage: www.elsevier.com/locate/foodchem

Influence of protein conformation and selected Hofmeister salts on bovine serum albumin/lutein complex formation

Paulo Henrique C. Paiva[a,b], Yara L. Coelho[c], Luis Henrique M. da Silva[c], Maximiliano S. Pinto[d], Márcia Cristina T.R. Vidigal[a], Ana Clarissa dos S. Pires[a,*]

[a] Grupo de Termodinâmica Molecular Aplicada, Departamento de Tecnologia de Alimentos, Av. PH Rolfs, s/n, Campus Universitário, Viçosa, MG 36570-900, Brazil
[b] Instituto de Laticínios Cândido Tostes, Empresa Agropecuária de Minas Gerais (EPAMIG), Rua Tenente Luiz de Freitas, 116, Santa Terezinha, Juiz de Fora, MG 36045-560, Brazil
[c] Grupo de Química Verde Coloidal e Macromolecular, Departamento de Química, Universidade Federal de Viçosa, Av. PH Rolfs, s/n, Campus Universitário, Viçosa, MG 36570-900, Brazil
[d] Instituto de Ciências Agrárias, Universidade Federal de Minas Gerais, Av. Universitária, 1000, Bairro Universitário, Montes Claros, MG 39404-547, Brazil

ARTICLE INFO

Chemical compounds studied in this article:
Lutein (PubChem CID: 5281243)
Warfarin (PubChem CID: 54678486)
Ibuprofen (PubChem CID: 3672)
Digitoxin (PubChem CID: 441207)
Sodium chloride (PubChem CID: 5234)
Sodium thiocyanate (PubChem CID: 516871)

Keywords:
Lutein
Bovine serum albumin
Complex formation
Fluorescence spectroscopy
Protein unfolding
Hofmeister salts
Thermodynamics

ABSTRACT

Protein conformation and the 3D water structure play important roles in the ability of bovine serum albumin (BSA) to form stable nanostructures with bioactive molecules. We studied the influence of BSA unfolding and those of two Hofmeister salts, sodium chloride (NaCl) as kosmotrope and sodium thiocyanate (NaSCN) as chaotrope, on BSA/lutein binding at pH 7.4 using fluorescence spectroscopy. The BSA/lutein complex formation was entropically driven and lutein was preferentially bound to site III of BSA. The binding constant (10^4 L mol^{-1}), complex stoichiometry (1:1), and thermodynamic potential for BSA/lutein binding were independent of protein conformation and Hofmeister salts. However, the enthalpic and entropic components of BSA/lutein binding in the presence of NaSCN decreased as the temperature increased. The opposite was observed for BSA/lutein binding in the presence of NaCl and for denatured BSA/lutein binding. Therefore, the BSA conformation and 3D water structure directly affected the BSA/lutein binding thermodynamics.

1. Introduction

The demand for natural and functional ingredients that contribute to consumers' well-being has grown recently. This trend is driven by the wide applications of carotenoids as natural colorants and bioactive ingredients in the food, nutraceutical, and cosmetic industries (Di Lena, Casini, Lucarini, & Lombardi-Boccia, 2018).

Lutein (Fig. 1) is a natural yellow-orange dye of the xanthophylls class, which are oxygenated carotenoids and generally co-exist with zeaxanthin (Kijlstra, Tian, Kelly, & Berendschot, 2012). Lutein is generally found in some leafy vegetables (e.g., spinach and kale), fruits (e.g., honeydew, mango, and watermelon), and egg yolk (Tan et al., 2016), and it has been recognized as an interesting food dye for the replacement of artificial dyes and development of functional foods (Sobral et al., 2016).

Several studies have reported the biological and pharmacological importance of lutein, such as its antioxidant and anti-inflammatory activity (Oh et al., 2013), mainly related to the prevention of age-related ocular diseases, including macular degeneration and cataracts (Kamoshita et al., 2016). However, its low aqueous solubility and bioavailability, as well as its sensitivity to heat, oxygen, and light are factors that limit the application of lutein in the food and pharmaceutical industries (Yi, Fan, Yokoyama, Zhang, & Zhao, 2016). To increase the physicochemical stability and aqueous solubility of lutein, its binding with different proteins has been studied (Chen et al., 2018; Mora-Gutierrez et al., 2018; Yi et al., 2016).

Yi et al. (2016) studied the binding of lutein with whey protein isolate (WPI) and sodium caseinate (SC) using circular dichroism, ultraviolet–visible (UV–vis) spectroscopy, and fluorescence spectroscopy at 25 °C and pH 7.4. Their results indicated that the complex formation

* Corresponding author.
E-mail address: ana.pires@ufv.br (A.C.d.S. Pires).

https://doi.org/10.1016/j.foodchem.2019.125463
Received 8 May 2019; Received in revised form 10 August 2019; Accepted 3 September 2019
Available online 06 September 2019
0308-8146/

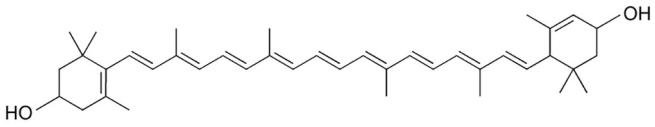

Fig. 1. Chemical structure of lutein.

between lutein and WPI or SC increased the stability of the carotenoid, and the stability of the SC/lutein complex was higher than that of the WPI/lutein one. However, WPI and SC are mixtures of proteins, i.e., WPI contains between 80 and 95 wt% whey proteins (mainly β-lactoglobulin, α-lactalbumin, and bovine serum albumin (BSA)) (Brans, Schroën, Van Der Sman, & Boom, 2004), while SC consists of four types of casein (α_{s1}-, α_{s2}-, β-, and κ-casein) (Holt, Carver, Ecroyd, & Thorn, 2013). Therefore, this study did not elucidate the individual contribution of each milk protein during their interactions with lutein. Mora-Gutierrez et al. (2018) investigated the binding of bovine and caprine caseins with lutein at pH 7.0 using UV–vis and fluorescence spectroscopy and confirmed that the aqueous solubility of lutein was improved owing to the casein/lutein complexes formation. Chen et al. (2018) studied the binding of carotenoids (isorenieratene, β-carotene, and lutein) with human serum albumin (HSA) at pH 7.4 using multi-spectroscopic methods and docking simulations. Their results suggested that HSA/carotenoids complexes formed and the binding processes were entropy- and enthalpy-driven.

Despite BSA being a model protein generally used for studying the binding of bioactive molecules (Rahman, Afrin, & Tabish, 2018), owing to its medical importance, abundance, easy purification, low cost, aqueous solubility, and stability (Shahabadi & Hadidi, 2014), to date, no studies were performed on BSA/lutein binding. However, some papers reported the formation of complexes between BSA and other carotenoids with structures similar to lutein. Li, Wang, Chen, and Lu (2015) investigated the binding thermodynamics of β-carotene and astaxanthin with HSA and BSA at pH 7.4, using spectroscopic techniques, and their results indicated that the proteins/carotenoids complex formation processes were enthalpically and entropically driven. Silva et al. (2018) studied the binding between β-carotene and native and denatured BSA using UV–vis and fluorescence spectroscopy at pH 7.0, and evidenced the complex formation between both BSA conformations and β-carotene, in addition to the improvement in photostability of the bioactive molecule. Allahdad, Varidi, Zadmard, Saboury, and Haertlé (2019) investigated the binding between β-carotene and whey proteins (β-lactoglobulin, α-lactalbumin, and BSA) as well as WPI, as function of pH, temperature, and sodium chloride (NaCl) concentration using spectroscopic techniques and docking studies. They demonstrated that β-carotene and whey proteins formed complexes with 1:1 stoichiometry, which were mainly driven by hydrophobic interactions, as binding weakened at low pH levels, ionic strengths, and temperatures.

Considering the relative similarity between lutein and β-carotene and the absence of thermodynamic data on the BSA/lutein complex formation, the goal of this study was to investigate the BSA/lutein binding process at pH 7.4. Moreover, the influence of the protein conformation and those of two Hofmeister salts (NaCl as kosmotrope and sodium thiocyanate (NaSCN) as chaotrope) on the binding thermodynamic parameters were also evaluated.

2. Materials and methods

2.1. Materials

Reagent grade BSA (> 98 wt%), ibuprofen (> 98 wt%), digitoxin (> 92 wt%), warfarin (> 99 wt%), NaCl (> 99.5 wt%), NaSCN (> 98 wt%), dimethyl sulfoxide (DMSO), dibasic sodium phosphate (Na_2HPO_4), and sodium phosphate monohydrate ($NaH_2PO_4{\cdot}H_2O$) were purchased from Sigma-Aldrich (St. Louis, MO, USA). Analytical grade, poly(ethylene oxide) (PEO) (molar mass 1500 g mol^{-1}) and lithium sulfate monohydrate ($Li_2SO_4{\cdot}H_2O$) (> 99 wt%) were purchased from Synth (São Paulo, SP, Brazil). Lutein (> 5 wt%) was kindly provided by DSM Nutritional Products (Kaiseraugst, AG, Switzerland). To prepare pH 7.4 buffer, we used Na_2HPO_4 (0.077 mol L^{-1}), $NaH_2PO_4{\cdot}H_2O$ (0.023 mol L^{-1}), and deionized water. No acids or bases were added to achieve the target pH.

2.2. Aqueous biphasic system extraction of lutein

Lutein (5 wt%) was purified using the aqueous biphasic system (ABS) comprising PEO (1500 g mol^{-1}) and Li_2SO_4 as electrolyte, according to the methodology adapted from Mageste et al. (2009) (see Fig. S1). The ABS was prepared using 25.506 g PEO solution (60 wt%) and 26.494 g Li_2SO_4 solution (23.8175 wt%). After the ABS reached equilibrium at 25 °C for 24 h the two phases were separated, and 8.0 g of each phase were mixed with 40 mg lutein (5 wt%) in glass tubes. These systems were mixed and maintained at 25 °C until they reached thermodynamic equilibrium. The concentrate orange interfaces were collected and centrifuged (Heraeus Fresco 21 Microcentrifuge, Thermo Fisher Scientific) at 2400 × *g* for 5 min at 8 °C. The precipitate was dispersed in deionized water and filtered using an UNIFIL (Germany) cellulose filter (12.5 cm in diameter and 0.20 mm thick) which retained particles 1 to 2 μm in size. Then, the filter was washed with deionized water (20 mL), and this procedure was repeated at least 10 times to remove all the PEO and Li_2SO_4 residues. The solid contents were collected and stored in a dark vial at freezing temperature for 24 h. Subsequently, the frozen sample was lyophilized using a SL-404 lyophilizer (SOLAB Laboratory Equipment, Brazil). The lyophilized sample was transferred to a dark vial and stored at freezing temperature.

The UV–vis and infrared spectra of the extracted lutein were recorded and compared with that of pure lutein (Silva et al., 2017).

2.3. Fluorescence spectroscopy

2.3.1. Determination of native and unfolding BSA/lutein binding

Fluorescence measurements were carried out on an LS55 fluorescence spectrophotometer (Perkin Elmer Inc., Waltham, USA), using quartz cells featuring the path length of 1 cm. Native or unfolding BSA solution (2.5 mL, 5 μM) in phosphate buffer (pH 7.4) containing 8% v/v DMSO was added to the cells. A unfolded BSA solution, without precipitation, was obtained by heating BSA at 80 °C for 10 min. Lutein was first dissolved in DMSO, and then was added to phosphate buffer (pH 7.4), so that the final volume of solvent (8% v/v) would not affect the protein fluorescence emission (Guercia, Forzato, Navarini, & Berti, 2016). Thus, a lutein stock solution (5.0×10^{-4} mol L^{-1}) was prepared, and series of 40 μL aliquots were added to the protein solution to achieve lutein concentrations between 0 and 57 μM (0, 8, 16, 23, 30, 37, 44, 50, and 57 μM). The excitation wavelength was 295 nm, the slit width for both excitation and emission was set to be 4 nm, and the emission spectra were recorded in the 296–450 nm wavelength range. Fluorescence quenching experiments were performed at five temperatures (25, 30, 35, 40, and 45 °C).

2.3.2. Determination of BSA preferential binding site for lutein

Competitive binding studies were performed using site probes for sites I, II, and III of BSA (warfarin, ibuprofen, and digitoxin, respectively). The concentrations of both BSA and site probes were constant (5 μM), and fluorescence quenching titration with lutein was performed as described above at pH 7.4 and 25 °C. Thus, the binding constant (K_b) for BSA/lutein was determined in the presence of site markers.

2.3.3. Determination of BSA/lutein binding at different Hofmeister salts concentrations

To evaluate the influence of two Hofmeister salts (NaCl and NaSCN) on the BSA/lutein binding process, native BSA solutions (5 μM) were

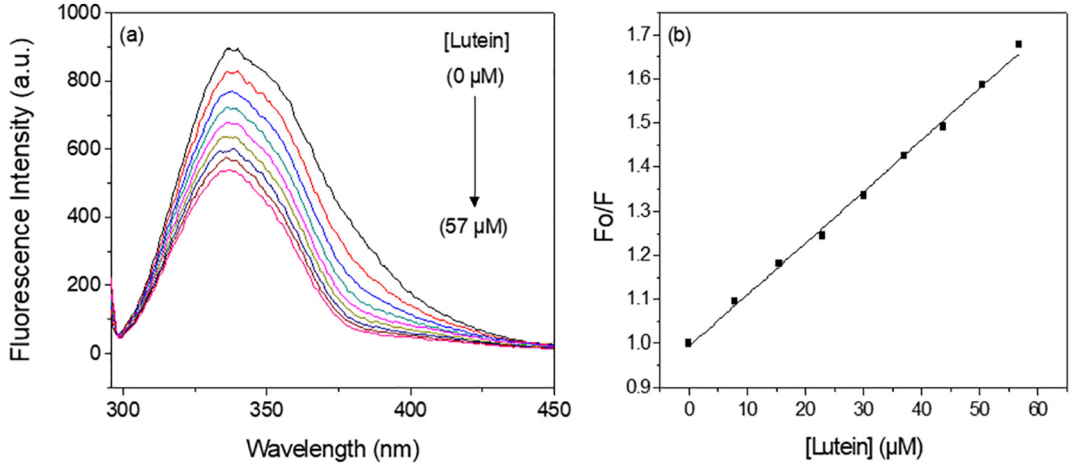

Fig. 2. (a) Fluorescence spectra of bovine serum albumin (5 μM) quenched with increasing concentrations of lutein at pH 7.4 (25 °C). The arrow indicates the increase in lutein concentration ([Lutein]) from 0 to 57 μM (0, 8, 16, 23, 30, 37, 44, 50, and 57 μM). (b) Stern–Volmer plot (F_0/F vs. lutein concentration) for fluorescence quenching of BSA induced by increasing concentrations of lutein. Here, F_0 and F are the fluorescence intensities of BSA in the absence and presence of quencher (lutein), respectively.

prepared in phosphate buffer (pH 7.4) containing 8% v/v DMSO as well as solutions of different concentrations (10, 50, and 70 mM) of the respective salts. Fluorescence quenching via lutein titration was performed as described in Section 2.3.1 above.

3. Results and discussion

3.1. Fluorescence spectroscopy study of BSA/lutein binding

Bovine serum albumin is a typical blood protein, which is also found in whey, and which contains two tryptophan (Trp) residues: Trp_{134} and Trp_{213}. These amino acid residues emit fluorescence when excited at 295 nm (Jahanban-Esfahlan, Panahi-Azar, & Sajedi, 2016). If BSA interacts with small molecules in the regions near the fluorophores, its intrinsic fluorescence decreases as the concentration of ligand increases (Lelis et al., 2017). Hence, fluorescence quenching is a suitable technique for studying the BSA/lutein binding process.

Fig. 2a presents the fluorescence spectra of BSA at pH 7.4 (25 °C), in the presence of increasing concentrations of lutein (0–57 μM). Similar results for the fluorescence quenching of BSA with lutein were obtained at other temperatures (Fig. S2A-a, A-b, A-c, and A-d).

The increase in lutein concentration induced a gradual decrease in the fluorescence intensity emitted by BSA. A small displacement in the maximum fluorescence emission wavelength ($\Delta\lambda_{em-max}$) which corresponded to the blue spectral region (338 to 335 nm) was noted, and indicated that Trp was driven toward the more hydrophobic environment. This small $\Delta\lambda_{em-max}$ displacement suggested that the BSA/lutein complex formation process was accompanied by a small conformational change in the structure of the protein.

Fluorescence quenching mechanisms can be classified as static or dynamic. The former occurs when a non-fluorescent protein–ligand complex is formed in the ground state. Conversely, dynamic quenching results from the collisional encounters between quencher and fluorophore (Ghosh, Rathi, & Arora, 2016).

The fluorescence quenching mechanism of BSA using lutein was defined using the Stern–Volmer equation (Eq. (1)):

$$\frac{F_0}{F} = 1 + K_q \tau_0 [Q] = 1 + K_{SV} [Q] \quad (1)$$

where F_0 and F are the fluorescence intensities of the protein (BSA) in the absence and presence of quencher (lutein), respectively, K_q is the quenching rate constant ($L\,mol^{-1}\,s^{-1}$), τ_0 is the average lifetime of protein without quencher (the fluorescence lifetime of biopolymers is 10^{-8} s), $[Q]$ is the quencher concentration ($mol\,L^{-1}$) and K_{SV} is the Stern–Volmer quenching constant ($L\,mol^{-1}$). When plotting F_0/F vs. $[Q]$, Eq. (1) can be used to determine the values of K_{SV} and K_q using linear regression (Lakowicz, 2006).

Dynamic and static quenching mechanisms can be distinguished using the dependence of K_{SV} on temperature. Generally, for dynamic quenching, K_{SV} increases as the temperature increases, but the reverse effect is observed for static quenching (Li et al., 2015). Another way to determine the fluorescence quenching mechanism involves using the K_q value. If K_q is $> 2 \times 10^{10}\,L\,mol^{-1}\,s^{-1}$, then the quenching mechanism is static (Lakowicz, 2006).

Fig. 2b illustrates the Stern–Volmer plot (F_0/F vs. $[Q]$) of the fluorescence quenching of BSA induced by increasing the concentration of lutein at pH 7.4 (25 °C). Stern–Volmer plots were also obtained at

Table 1
Fluorescence quenching constant (K_{SV}), binding constant (K_b), and stoichiometric coefficient of lutein (n) for bovine serum albumin/lutein binding at pH 7.4.

Protein	T (°C)	K_{SV} ($\times 10^4\,L\,mol^{-1}$)	R^2	K_b ($\times 10^4\,L\,mol^{-1}$)	n	R^2
Native	25	1.13 ± 0.05	0.9971	1.14 ± 0.05	1.00 ± 0.03	0.9954
	30	1.10 ± 0.02	0.9915	1.23 ± 0.01	1.24 ± 0.02	0.9994
	35	1.09 ± 0.04	0.9887	1.25 ± 0.06	1.30 ± 0.03	0.9996
	40	1.07 ± 0.02	0.9880	1.30 ± 0.06	1.43 ± 0.15	0.9952
	45	1.00 ± 0.12	0.9830	1.34 ± 0.05	1.62 ± 0.14	0.9865
Denatured	25	1.08 ± 0.10	0.9962	1.13 ± 0.12	1.09 ± 0.03	0.9981
	30	1.01 ± 0.15	0.9959	1.13 ± 0.12	1.17 ± 0.06	0.9984
	35	1.03 ± 0.08	0.9917	1.16 ± 0.04	1.24 ± 0.04	0.9996
	40	1.00 ± 0.14	0.9915	1.22 ± 0.06	1.35 ± 0.13	0.9913
	45	0.95 ± 0.11	0.9895	1.23 ± 0.04	1.46 ± 0.18	0.9909

R^2 is the determination coefficient. All K_{SV}, K_b, and n values are means ± standard deviations for two sets of measurements.

other temperatures (Fig. S2B).

The K_{SV} values for BSA/lutein binding decreased from 1.13×10^4 to $1.00 \times 10^4\,L\,mol^{-1}$ when the temperature increased from 25 to 45 °C (Table 1).

Considering K_{SV} to be $10^4\,L\,mol^{-1}$, all K_q values were at least 100 times higher than $10^{10}\,L\,mol^{-1}\,s^{-1}$ ($10^{12}\,L\,mol^{-1}\,s^{-1}$), which ensured that BSA/lutein complex formation was the predominant fluorescence quenching mechanism of BSA by lutein.

For the static quenching process, it was considered that lutein was bound to "n" equivalent and independent protein binding sites i.e., all binding sites presented the same capacity for BSA/lutein binding. The equilibrium reaction can be written as:

$$BSA + nL \rightleftarrows L_n(BSA)$$

where L is the lutein molecule and L_n(BSA) is the BSA/lutein complex. The binding constant of the L_n(BSA) complex is K_b (Bi et al., 2004).

We determined the equilibrium binding constant (K_b) and stoichiometric coefficient of lutein (n) for the BSA/lutein complex using the Scatchard (double log regression curve) equation (Eq. (2), Fig. S10a) (Ksenofontov, Bocharov, & Antina, 2019):

$$log\frac{F_0 - F}{F} = nlogK_b - nlog\frac{1}{[Q_t] - \frac{(F_0 - F)}{F_0}[BSA]} \quad (2)$$

where $[Q_t]$ and $[BSA]$ are the total lutein and BSA concentrations, respectively. The n and K_b values were obtained from the slope and intercept of the $log\frac{F_0-F}{F}$ vs. $log\frac{1}{[Q_t]-\frac{(F_0-F)}{F_0}[BSA]}$ curve, respectively.

The complex presented 1:1 stoichiometry, i.e., one lutein molecule for each BSA binding site. Moreover, K_b slightly increased as the temperature increased, ranging from 1.14×10^4 to $1.34 \times 10^4\,L\,mol^{-1}$ (Table 1), which indicated that the complex formation was an endothermic thermodynamic process.

Chen et al. (2018) determined that the K_b value for HSA/lutein binding at pH 7.4 and 25 °C was $2.14 \times 10^5\,L\,mol^{-1}$ which was 19 times higher than for the BSA/lutein binding at 25 °C ($1.14 \times 10^4\,L\,mol^{-1}$). Li et al. (2015) also reported differences in the K_b values for the binding of other carotenoids with HSA and BSA, and the K_b values for HSA and BSA binding with astaxanthin and β-carotene decreased as follows: HSA/astaxanthin > BSA/astaxanthin = HSA/β-carotene > BSA/β-carotene. Therefore, HSA/carotenoid binding appeared to be stronger than BSA/carotenoid binding, and despite the similarities between HSA and BSA, these proteins displayed different binding properties (Bou-Abdallah, Sprague, Smith, & Giffune, 2016; Dawoud Bani-Yaseen, 2011).

The structure of lutein can be described as a long carbon chain featuring alternating C—C and C=C bonds with attached methyl side groups. At both ends of the carbon backbone, the molecule contains cyclic hexenyl structures with attached hydroxyl groups (Kijlstra et al., 2012). Hence, lutein could interact with different BSA sites. To identify the preferential interaction site for the lutein–BSA interaction, a competitive binding experiment with specific markers was performed.

Sites I, II, and III of BSA corresponded to its IIA, IIIA, and IB subdomains, respectively (Rahman et al., 2018). Warfarin is known to bind specifically onto site I of BSA, while ibuprofen and digitoxin are markers for sites II and III of BSA, respectively (Datta, Mahapatra, & Halder, 2013). Thus, competitive binding experiments were conducted using these three markers to identify the BSA preferential binding site for lutein. The changes in K_b with the added site markers for the BSA/lutein system, φ, was determined using Eq. (3) (Chen et al., 2018):

$$\varphi = \frac{K_b' - K_b}{K_b} \quad (3)$$

where K_b' and K_b are the binding constant of the BSA/lutein complex formation in the presence and absence of site markers, respectively.

For BSA/lutein binding, K_b decreased more in the presence of digitoxin ($\varphi = -8.77\%$), compared with ibuprofen ($\varphi = -2.63\%$) and warfarin ($\varphi = -0.88\%$) (Table S1). These results suggested that lutein bound primarily to site III of BSA. Binding site III consists of hydrophobic residues such as proline 117, isoleucine 181, leucine 115, tyrosine 137, valine 188, leucine 122, and isoleucine 141 (Rahman et al., 2018), which indicated that hydrophobic interactions were the major players in conferring stability to the BSA/lutein complex. Nevertheless, site III also presents Tyr 160 and glutamic acid 140 residues (Rahman et al., 2018), which probably formed hydrogen bonds with the hydroxyl (OH) groups at each end of the lutein polyene chain.

3.2. Thermodynamic analysis of BSA/lutein binding

In addition to identifying the binding site for lutein on BSA, the understanding of the main forces driving the BSA/lutein binding could help optimize the thermodynamic conditions for the transport of lutein by BSA. Thus, we determined the following thermodynamic parameters for BSA/lutein binding: standard Gibbs free energy, enthalpy, entropy, and heat capacity changes (ΔG°, ΔH°, ΔS°, and ΔC_p°, respectively).

To obtain the ΔH° values, we used a polynomial model (Eq. (4)) to derive the nonlinear van't Hoff equation (Eq. (5)) (Da Silva et al., 2008):

$$ln\,K_b = a + b\left(\frac{1}{T}\right) + c\left(\frac{1}{T}\right)^2 + d\left(\frac{1}{T}\right)^3 + \ldots ln\,\phi \quad (4)$$

$$\Delta H^\circ = -R\frac{dlnK_b}{d\left(\frac{1}{T}\right)} \rightarrow \Delta H^\circ = -R\left[b + 2c\left(\frac{1}{T}\right) + 3d\left(\frac{1}{T}\right)^2 + \ldots\right] \quad (5)$$

where a, b, c, d, and $ln\phi$ are constants, which can be graphically determined using the polynomial adjust, R is the universal constant of ideal gases ($8.3145\,J\,mol^{-1}\,K^{-1}$), and T is the temperature (K).

Fig. 3a presents the nonlinear van't Hoff plot for the determination of ΔH° of the BSA/lutein complex formation at pH 7.4.

The ΔG° and $T\Delta S^\circ$ values were calculated using Eqs. (6) and (7), respectively.

$$\Delta G^\circ = -RTlnK_b \quad (6)$$

$$\Delta G^\circ = \Delta H^\circ - T\Delta S° \quad (7)$$

where the measurement units for ΔG° and ΔS° were $kJ\,mol^{-1}$ and $kJ\,mol^{-1}\,K^{-1}$, respectively.

Table 2 presents the thermodynamic parameters for the BSA/lutein binding at pH 7.4.

The ΔG° values were negative and slightly decreased as the temperature increased, which indicated that the BSA/lutein complexes were more stable than the free BSA and lutein molecules for all temperature ranges. Moreover, the higher the temperature the more stable the complexes. Silva et al. (2018) determined that the ΔG° values ranged from -28.96 to $-31.65\,kJ\,mol^{-1}$ for the BSA/β-carotene binding at pH 7.0, in the same temperature range (25–45 °C). Hence, both studies revealed similar behaviors for the two carotenoids that interacted with BSA.

The ΔH° and $T\Delta S^\circ$ values for the BSA/lutein complex formation were positive, which indicated that the hydrophobic effect drove the BSA/lutein binding process. However, this effect decreased as the temperature increased, mainly owing to the decrease in the organization of 3D water structure, which diminished the ΔH° and $T\Delta S^\circ$ contributions.

To explain the magnitude of the ΔH° values of the BSA/lutein complex formation process, ΔH° should be considered to be the sum of terms associated with three molecular processes: desolvation of BSA and lutein surfaces (ΔH_{des}°), conformational change of BSA binding site (ΔH_{conf}°), and BSA/lutein interaction (ΔH_{int}°) (Eq. (8)):

$$\Delta H^\circ = \Delta H_{des}^\circ + \Delta H_{conf}^\circ + \Delta H_{int}^\circ \quad (8)$$

The desolvation of BSA and lutein surfaces involves breaking the water–water interactions from the solvation layers of interacting molecules and formation of water–water bonds in the bulk, and therefore, ΔH_{des}° is always positive because the hydrophobic effect predominates.

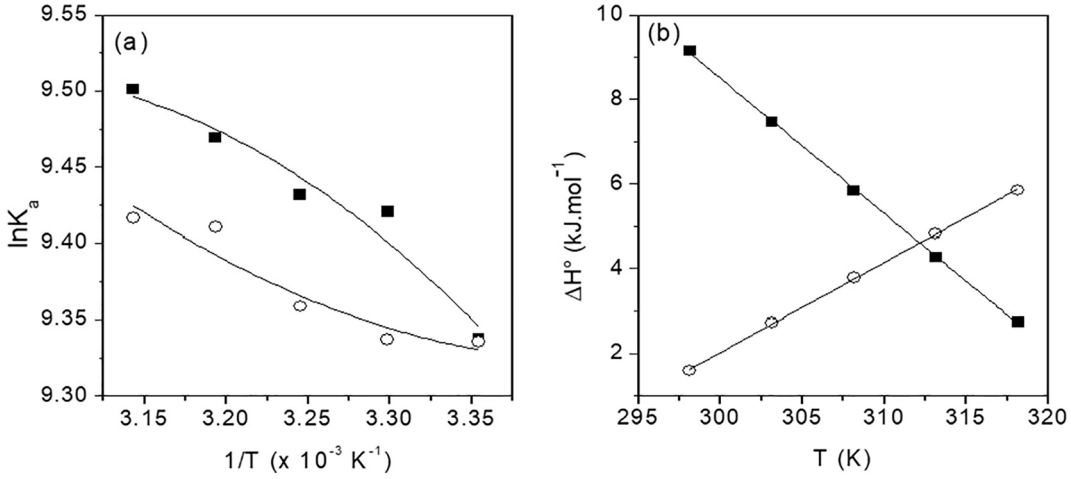

Fig. 3. (a) Nonlinear van't Hoff plot for determination of standard enthalpy change (ΔH°) and (b) plot of ΔH° vs. temperature (T) for determination of the standard heat capacity change (ΔC_p°) of BSA/lutein (closed symbols) and denatured BSA/lutein (open symbols) complexes formation at pH 7.4.

Table 2
Standard enthalpy, Gibbs free energy, and entropic term changes (ΔH°, ΔG°, and $T\Delta S^{\circ}$, respectively) for bovine serum albumin/lutein complex formation at pH 7.4, which were obtained using fluorescence studies.

T (°C)	ΔH° (kJ mol^{-1})	R^2	ΔG° (kJ mol^{-1})[a]	$T\Delta S^{\circ}$ (kJ mol^{-1})[b]
25	9.14	0.96	−23.15	32.29
30	7.46		−23.74	31.20
35	5.84		−24.16	30.00
40	4.26		−24.65	28.92
45	2.74		−25.13	27.87

R^2 is the determination coefficient. ΔH°, ΔG°, and $T\Delta S^{\circ}$ values are means from two sets of measurements.
[a] Standard deviation lower than 1%.
[b] Standard deviation lower than 10%.

The ΔH_{conf}° value is also positive owing to the breakdown of the intramolecular bonds between amino acids residues, while ΔH_{int}° is always negative owing to the energy released during the BSA/lutein interaction.

The same analysis could be performed for the entropic term, and the total entropic contribution associated with BSA/lutein binding could be expressed as the sum of three terms (Eq. (9)):

$$T\Delta S^{\circ} = T\Delta S_{des}^{\circ} + T\Delta S_{conf}^{\circ} + T\Delta S_{int}^{\circ} \quad (9)$$

where ΔS_{des}° is the standard entropy change associated with the solvent release during BSA/lutein binding, which is always positive, ΔS_{conf}° is the entropy change associated with the conformational change of BSA binding site, and can be negative (if the interaction yields a more structured site) or positive (if the protein-ligand binding disrupts the site), and ΔS_{int}° is the standard entropy change related to the BSA/lutein interaction, which is always negative because the complex presents lower configurational entropy than the free BSA and lutein molecules.

The $T\Delta S_{des}^{\circ}$ values decreased as the temperature increased owing to the smaller structural differences between the solvation water molecules and those present in the bulk at higher temperature. As $T\Delta S^{\circ}$ depended on three simultaneously occurring processes and the difference between $|T\Delta S_{des}^{\circ}|$ and $|T\Delta S_{conf}^{\circ}|$ decreased as the temperature increased, consequently, $T\Delta S^{\circ}$ decreased.

The ΔC_p° values for the BSA/lutein complexation process were determined from the temperature dependence of ΔH° using Eq. (10):

$$\Delta C_p^{\circ} = \frac{\partial(\Delta H^{\circ})}{\partial T} \quad (10)$$

According to Bou-Abdallah et al. (2016), ΔC_p° could provide insights into changes in structure and energy pertaining to solvent reorganization (i.e., hydration–dehydration events) that accompany ligand–protein interactions. Fig. 3b illustrates the decrease in ΔH° with the increase in temperature for the BSA/lutein complex formation process.

The ΔC_p° value associated with the BSA/lutein complex formation was negative ($\Delta C_p^{\circ} = -0.32\,\text{kJ mol}^{-1}\,\text{K}^{-1}$, $R^2 = 0.9995$). Considering that $\Delta C_p^{\circ} = C_{p(BSA/lutein)}^{\circ} - (C_{p(BSA)}^{\circ} + C_{p(lutein)}^{\circ})$, the negative ΔC_p° value indicated that the magnitude of the intermolecular interactions that formed in the BSA/lutein complex was smaller than that of the interactions occurring when the BSA and lutein molecules were in the free form. Negative ΔC_p° values are generally associated with changes in hydrophobic or polar group hydration where dominant hydrophobic forces are involved in binding, and suggest that the ligand–protein complex formation is accompanied by the burial of hydrophobic groups and desolvation of interacting molecules (Bou-Abdallah et al., 2016). This result corroborated the positive ΔH° and $T\Delta S^{\circ}$ values determined before and reinforced the role of the desolvation process during BSA/lutein binding.

3.2.1. *Influence of protein conformation on BSA/lutein binding*

Proteins can unfold when exposed to high temperatures. As most foods are thermally treated, it is relevant to investigate the binding between bioactive molecules, such as lutein, and denatured proteins.

The fluorescence spectra of unfolded BSA (without lutein) exhibited the λ_{em-max} at 333 nm, which was smaller than that of the native protein. This result corroborated our hypothesis that the BSA/lutein interaction caused conformation changes in the binding site of the macromolecule. Additionally, BSA unfolding drove the Trp residue toward the more hydrophobic environment (Suryawanshi, Walekar, Gore, Anbhule, & Kolekar, 2016).

The fluorescence intensity of denatured BSA (BSA_{den}) was quenched by lutein (Fig. S3A-a, A-b, A-c, A-d, A-e). Analysis of the fluorescence data yielded K_b values for BSA_{den}/lutein binding ranging from 1.13×10^4 to $1.23 \times 10^4\,\text{L mol}^{-1}$, which were very close to the K_b values obtained for native BSA/lutein binding. The influence of protein unfolding on the stoichiometry of the complex formation process was almost negligible (Table 1 and Fig. S10b). These results suggested that although lutein binds preferentially to site III of BSA, site conformation does not affect the BSA/lutein interaction considerably. We hypothesized that, after denaturation, BSA exposed its hydrophobic groups, which aggregated and provided hydrophobic regions to carry lutein (Militello, Vetri, & Leone, 2003).

The stabilities of the BSA_{den}/lutein complexes, expressed using ΔG° values, remained almost the same as those of the native BSA/lutein complexes. Moreover, the BSA_{den}/lutein complex formation was driven

by the hydrophobic effect since the ΔH° and $T\Delta S^{\circ}$ values remained positive despite protein unfolding (Table S2).

The ΔH° and $T\Delta S^{\circ}$ values increased as the temperature increased, because the higher the temperature, the higher the ΔH_{conf}° and ΔS_{conf}° values of the binding site for lutein on BSA_{den}. Considering that even though the quenching mechanism responsible for BSA_{den}/lutein complex formation is still the static quenching, intermolecular collisions between the protein and the bioactive molecule occurs in the system. Thus, the temperature effect on the ΔH° and $T\Delta S^{\circ}$ values could be attributed to the larger amounts of kinetic energy being transferred to molecules by collisions at high temperatures, which overcame the rotational barrier of the protein. Hence, the binding site for lutein on BSA_{den} became more flexible as the temperature increased, which increased the energy costs and system entropy.

While ΔC_p° for BSA/lutein binding was negative, ΔC_p° was positive for the BSA_{den}/lutein complex formation ($\Delta C_p^{\circ} = 0.21\ kJ\ mol^{-1}\ K^{-1}$, $R^2 = 0.9995$), which suggested that stronger interactions occurred in the system when the BSA_{den}/lutein complex was formed. Fig. 3b illustrates the increase in ΔH° with the increase in temperature for the BSA_{den}/lutein complex formation process. Considering the increase in flexibility of the binding site of BSA_{den} for lutein, more amino acid residues were exposed and were consequently available to interact with the bioactive molecule mainly through hydrophobic interactions (Hudson et al., 2018), which corroborated the hypothesis of the conformational-induced fit to the ΔH° and $T\Delta S^{\circ}$ increase with temperature.

3.2.2. Influence of selected Hofmeister series salts on native BSA/lutein binding

The effective utilization of BSA as lutein carrier depends extensively on its properties in different thermodynamic media, and factors such as the pH, temperature, and ionic strength. Ionic strength could influence the conformation and double electric layer of proteins as well as the 3D structure of water, and therefore could mainly affect the hydrophobic and electrostatic interactions (Wang & Arnt, 2015). Therefore, the influence of different concentrations of two Hofmeister salts: NaCl (kosmotropic) and NaSCN (chaotropic) were studied for the BSA/lutein binding process.

Independent of salt addition (NaCl or NaSCN), the emission spectra of the BSA solution indicated that the increase in lutein concentration resulted in the gradual decrease in protein fluorescence intensity (Figs. S4–S6 and S7–S9, for NaCl and NaSCN, respectively). The K_q values of approximately $10^{12}\ L\ mol^{-1}\ s^{-1}$ were unchanged, which indicated that despite the presence of the chaotropic or kosmotropic salt, the fluorescence quenching mechanism of BSA by lutein was due to the BSA/lutein complex formation.

The influence of the salts on K_b and n were almost negligible, and K_b and n were approximately $10^4\ L\ mol^{-1}$ and 1.0, respectively (Table S3 and Fig. S10c–h). Additionally, the $\Delta\lambda_{em-max}$ value was the same as that observed in the native BSA spectrum owing to its interaction with lutein, which corresponded to the blue spectral region from 338 to 335 nm. Hence, we concluded that the presence of the salts did not affect the binding site for lutein on BSA.

The ΔG° values for BSA/lutein complex formation in the presence of NaCl and NaSCN solutions of different concentrations were negative and remained almost unchanged as the temperature increased (Table S3). Thermodynamic processes where ΔG° is rather independent of temperature occur generally via entropy–enthalpy compensation (EEC). The EEC phenomenon implies that the change in enthalpy could be partially or fully offset by the change in entropy: $\Delta\Delta H^{\circ} \approx T\Delta\Delta S^{\circ}$ and $\Delta\Delta G^{\circ} \approx 0$ (Bou-Abdallah et al., 2016), which generally hydrophobic forces are important during the compensation process. When EEC occurs, the plots of ΔH° and ΔG° vs. $T\Delta S^{\circ}$ yield straight lines (Basu & Kumar, 2014). The slopes of the ΔH° vs. $T\Delta S^{\circ}$ plots were 1.08, 1.08, and 1.09, respectively, for the NaSCN concentrations of 10, 50, and 70 mM, respectively, while the slopes of the ΔG° vs. $T\Delta S^{\circ}$ plots were 0.09, 0.08 and 0.08, respectively, for the same concentrations. The slopes of the

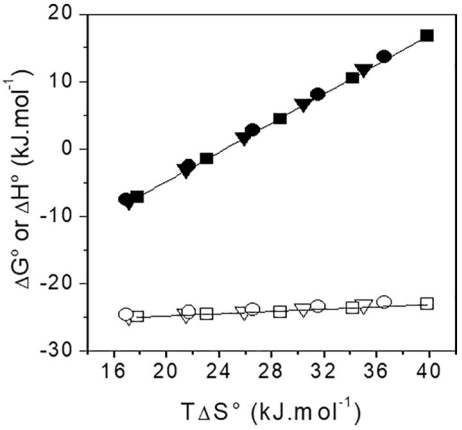

Fig. 4. Changes in Gibbs free energy (ΔG°) (open symbols) and enthalpy (ΔH°) (closed symbols) as functions of entropic term ($T\Delta S^{\circ}$) for bovine serum albumin/lutein binding at pH 7.4 and NaSCN concentrations of (▼,▽) 10, (■,□) 50, and (●,○) 70 mM.

ΔH° vs. $T\Delta S^{\circ}$ plots were near unity, while the slopes of the ΔG° vs. $T\Delta S^{\circ}$ plots were close to zero, which indicated the occurrence of EEC in these systems. The EEC for BSA/lutein binding in the presence of 10, 50, and 70 mM NaSCN was evidenced in the ΔG° and ΔH° vs. $T\Delta S^{\circ}$ plots (Fig. 4).

No EEC occurred for the BSA/lutein binding process in the absence of salts (when native or denatured BSA was used) or in the presence of NaCl at any concentration (10, 50, or 70 mM).

Even though the salts did not affect the thermodynamic potential (ΔG°) of the BSA/lutein binding process, the electrolytes significantly affected the ΔH° and $T\Delta S^{\circ}$ parameters.

The BSA/lutein complexation at NaCl concentrations of 10, 50, and 70 mM was driven by the increase in entropy, and the ΔH° and $T\Delta S^{\circ}$ values became more positive as the temperature increased (Table S3). This behavior could be explained considering that NaCl increased the organization of 3D water structure (Hyde et al., 2017), which decreased the ΔH_{des}° values compared with that obtained for the salt-free system. In the presence of NaCl, the structural and energetic differences between water molecules in the bulk and those solvating hydrophobic molecular surfaces decreased.

Fig. S12a depicts the ΔH° vs. temperature plot that was used to calculate the ΔC_p° values, which, unlike those calculated in the absence of salts, were positive: 0.96, 0.70, and 0.30 $kJ\ K^{-1}\ mol^{-1}$ for BSA/lutein binding at NaCl concentrations of 10, 50, and 70 mM, respectively. The positive ΔC_p° values for BSA/lutein binding suggested that the presence of NaCl caused the intramolecular interactions inside the complex to become stronger than those that occurred in the salt-free system.

As NaSCN is a chaotropic salt, its influence on the thermodynamic parameters were the opposite of those observed for NaCl. The ΔH° and $T\Delta S^{\circ}$ values for BSA/lutein binding decreased as the temperature increased at all analyzed NaSCN concentrations (10, 50, and 70 mM) (Table S3).

Fig. S12b presents the ΔH° vs. temperature plot, which was used to calculate the influence of NaSCN on the ΔC_p°. Unlike NaCl, NaSCN was able to decrease the organization of 3D water structure (Hyde et al., 2017), which yielded negative ΔC_p° values (-0.98, -1.20 and $-1.06\ kJ\ mol^{-1}\ K^{-1}$) for BSA/lutein binding at the NaSCN concentrations of 10, 50, and 70 mM, respectively. The negative ΔC_p° values at different NaSCN concentrations suggested that the intermolecular interactions that formed were weaker than those broken during the complex formation process.

4. Conclusions

The results of this study suggested that lutein and BSA form a

complex with 1:1 binding stoichiometry, which is driven by hydrophobic interactions regardless of protein unfolding and presence of selected Hofmeister salts. Site marker experiments revealed that lutein bound preferentially to site III of BSA. The stabilities of the BSA/lutein complex, which were expressed using ΔG° values, remained almost unchanged under all analyzed conditions. On the other hand, the protein conformation and salts influenced the ΔG° components, i.e., ΔH° and $T\Delta S^{\circ}$, as well as the ΔC_p° values. The ΔH° and $T\Delta S^{\circ}$ values for BSA/lutein binding were positive and decreased as the temperature increased, and consequently resulted in negative ΔC_p° values. This suggests that the complexation process was accompanied by burial of hydrophobic groups and desolvation of interacting molecules. The positive ΔC_p° values for BSA_{den}/lutein binding indicated the increased exposure and availability of the hydrophobic amino acids of the protein for interacting with the lutein molecule. NaCl increased the organization of 3D water structure and consequently decreased the ΔH° values compared with that of the salt-free system. In addition, the positive ΔC_p° values for BSA/lutein binding at different NaCl concentrations suggested that the intramolecular interactions present inside the complex were stronger than those that occurred in the absence of the salt. On the other hand, NaSCN solutions of different concentrations decreased the organization of 3D water structure and resulted in negative ΔC_p° values, which indicated that the intermolecular interactions formed in the presence of NaSCN were weaker than those broken during the BSA/lutein complex formation process. Thus, the protein conformation and 3D water structure play important roles on BSA/lutein binding, as evidenced by the influence of protein unfolding and selected Hofmeister salts on the thermodynamic binding parameters. These data, taken together, suggest that the high hydrophobicity of lutein is involved in the binding of BSA.

Declaration of competing interest

The authors declare that they have no known competing financial interests or personal relationships that could have appeared to influence the work reported in this paper.

Acknowledgments

The authors thank the Coordenação de Aperfeiçoamento de Pessoal de Nível Superior (CAPES), Conselho Nacional de Desenvolvimento Científico e Tecnológico (CNPq) and Fundação de Apoio à Pesquisa de Minas Gerais (FAPEMIG) for their financial support, and the DSM Nutritional Products for kindly providing lutein.

Appendix A. Supplementary data

Supplementary data to this article can be found online at https://doi.org/10.1016/j.foodchem.2019.125463.

References

Allahdad, Z., Varidi, M., Zadmard, R., Saboury, A. A., & Haertlé, T. (2019). Binding of β-carotene to whey proteins: Multi-spectroscopic techniques and docking studies. *Food Chemistry, 277*, 96–106. https://doi.org/10.1016/j.foodchem.2018.10.057.

Basu, A., & Kumar, G. S. (2014). Study on the interaction of the toxic food additive carmoisine with serum albumins: A microcalorimetric investigation. *Journal of Hazardous Materials, 273*, 200–206. https://doi.org/10.1016/j.jhazmat.2014.03.049.

Bi, S., Ding, L., Tian, Y., Song, D., Zhou, X., Liu, X., & Zhang, H. (2004). Investigation of the interaction between flavonoids and human serum albumin. *Journal of Molecular Structure, 703*(1–3), 37–45. https://doi.org/10.1016/j.molstruc.2004.05.026.

Bou-Abdallah, F., Sprague, S. E., Smith, B. M., & Giffune, T. R. (2016). Binding thermodynamics of diclofenac and naproxen with human and bovine serum albumins: A calorimetric and spectroscopic study. *Journal of Chemical Thermodynamics, 103*, 299–309. https://doi.org/10.1016/j.jct.2016.08.020.

Brans, G., Schroën, C. G. P. H., Van Der Sman, R. G. M., & Boom, R. M. (2004). Membrane fractionation of milk: State of the art and challenges. *Journal of Membrane Science, 243*(1–2), 263–272. https://doi.org/10.1016/j.memsci.2004.06.029.

Chen, Y., Zhou, Y., Chen, M., Xie, B., Yang, J., Chen, J., & Sun, Z. (2018). Isorenieratene interaction with human serum albumin: Multi-spectroscopic analyses and docking simulation. *Food Chemistry, 258*(November 2017), 393–399. https://doi.org/10.1016/j.foodchem.2018.02.105.

Da Silva, L. H. M., Da Silva, M. C. H., Francisco, K. R., Cardoso, M. V. C., Minim, L. A., & Coimbra, J. S. R. (2008). PEO-[M(CN)5NO]x-(M═Fe, Mn, or Cr) interaction as a driving force in the partitioning of the pentacyanonitrosylmetallate anion in ATPS: Strong effect of the central atom. *Journal of Physical Chemistry B, 112*(37), 11669–11678. https://doi.org/10.1021/jp711617z.

Datta, S., Mahapatra, N., & Halder, M. (2013). pH-insensitive electrostatic interaction of carmoisine with two serum proteins: A possible caution on its uses in food and pharmaceutical industry dedicated to professor Mihir Chowdhury. *Journal of Photochemistry and Photobiology B: Biology, 124*, 50–62. https://doi.org/10.1016/j.jphotobiol.2013.04.004.

Dawoud Bani-Yaseen, A. (2011). Spectrofluorimetric study on the interaction between antimicrobial drug sulfamethazine and bovine serum albumin. *Journal of Luminescence, 131*(5), 1042–1047. https://doi.org/10.1016/j.jlumin.2011.01.019.

Di Lena, G., Casini, I., Lucarini, M., & Lombardi-Boccia, G. (2018). Carotenoid profiling of five microalgae species from large-scale production. Food Research International, (July 2018), 1–9. doi:https://doi.org/10.1016/j.foodres.2018.11.043

Ghosh, K., Rathi, S., & Arora, D. (2016). Fluorescence spectral studies on interaction of fluorescent probes with bovine serum albumin (BSA). *Journal of Luminescence, 175*, 135–140. https://doi.org/10.1016/j.jlumin.2016.01.029.

Guercia, E., Forzato, C., Navarini, L., & Berti, F. (2016). Interaction of coffee compounds with serum albumins. Part II: Diterpenes. *Food Chemistry, 199*, 502–508. https://doi.org/10.1016/j.foodchem.2015.12.051.

Holt, C., Carver, J. A., Ecroyd, H., & Thorn, D. C. (2013). Invited review: Caseins and the casein micelle: Their biological functions, structures, and behavior in foods. *Journal of Dairy Science, 96*(10), 6127–6146. https://doi.org/10.3168/jds.2013-6831.

Hudson, E. A., de Paula, H. M. C., Ferreira, G. M. D., Ferreira, G. M. D., Hespanhol, M.d. C., da Silva, L. H. M., & Pires, A. C.d. S. (2018). Thermodynamic and kinetic analyses of curcumin and bovine serum albumin binding. *Food Chemistry, 242*(June 2017), 505–512. https://doi.org/10.1016/j.foodchem.2017.09.092.

Hyde, A. M., Zultanski, S. L., Waldman, J. H., Zhong, Y. L., Shevlin, M., & Peng, F. (2017). General principles and strategies for salting-out informed by the Hofmeister series. *Organic Process Research and Development, 21*(9), 1355–1370. https://doi.org/10.1021/acs.oprd.7b00197.

Jahanban-Esfahlan, A., Panahi-Azar, V., & Sajedi, S. (2016). Interaction of glutathione with bovine serum albumin: Spectroscopy and molecular docking. *Food Chemistry, 202*, 426–431. https://doi.org/10.1016/j.foodchem.2016.02.026.

Kamoshita, M., Toda, E., Osada, H., Narimatsu, T., Kobayashi, S., Tsubota, K., & Ozawa, Y. (2016). Lutein acts via multiple antioxidant pathways in the photo-stressed retina. *Scientific Reports, 6*(July), 1–10. https://doi.org/10.1038/srep30226.

Kijlstra, A., Tian, Y., Kelly, E. R., & Berendschot, T. T. J. M. (2012). Lutein: More than just a filter for blue light. *Progress in Retinal and Eye Research, 31*(4), 303–315. https://doi.org/10.1016/j.preteyeres.2012.03.002.

Ksenofontov, A. A., Bocharov, P. S., & Antina, E. V. (2019). Interaction of tetramethyl-substituted BODIPY dye with bovine serum albumin: Spectroscopic study and molecular docking. *Journal of Photochemistry and Photobiology A: Chemistry, 368*(September 2018), 254–257. https://doi.org/10.1016/j.jphotochem.2018.10.002.

Lakowicz, J. R. (2006). *Principles of fluorescence spectroscopy*. New York: Springer.

Lelis, C. A., Hudson, E. A., Ferreira, G. M. D., Ferreira, G. M. D., da Silva, L. H. M., Silva, d., ... Pires, A. C. S. (2017). *Binding thermodynamics of synthetic dye Allura Red with bovine serum albumin. Food Chemistry, 217*, 52–58. https://doi.org/10.1016/j.foodchem.2016.08.080.

Li, X., Wang, G., Chen, D., & Lu, Y. (2015). β-Carotene and astaxanthin with human and bovine serum albumins. *Food Chemistry, 179*, 213–221. https://doi.org/10.1016/j.foodchem.2015.01.133.

Mageste, A. B., de Lemos, L. R., Ferreira, G. M. D., Silva, d., do CH, M., da Silva, L. H. M., ... Minim, L. A. (2009). *Aqueous two-phase systems: An efficient, environmentally safe and economically viable method for purification of natural dye carmine. Journal of Chromatography A, 1216*(45), 7623–7629. https://doi.org/10.1016/j.chroma.2009.09.048.

Militello, V., Vetri, V., & Leone, M. (2003). Conformational changes involved in thermal aggregation processes of bovine serum albumin. *Biophysical Chemistry, 105*(1), 133–141. https://doi.org/10.1016/S0301-4622(03)00153-4.

Mora-Gutierrez, A., Attaie, R., Núñez de González, M. T., Jung, Y., Woldesenbet, S., & Marquez, S. A. (2018). Complexes of lutein with bovine and caprine caseins and their impact on lutein chemical stability in emulsion systems: Effect of arabinogalactan. *Journal of Dairy Science, 101*(1), 18–27. https://doi.org/10.3168/jds.2017-13105.

Oh, J., Kim, J. H., Park, J. G., Yi, Y. S., Park, K. W., Rho, H. S., & Cho, J. Y. (2013). Radical scavenging activity-based and AP-1-targeted anti-inflammatory effects of lutein in macrophage-like and skin keratinocytic cells. *Mediators of Inflammation, 2013*(August), https://doi.org/10.1155/2013/787042.

Rahman, Y., Afrin, S., & Tabish, M. (2018). Interaction of pirenzepine with bovine serum albumin and effect of β-cyclodextrin on binding: A biophysical and molecular docking approach. *Archives of Biochemistry and Biophysics, 652*(June), 27–37. https://doi.org/10.1016/j.abb.2018.06.005.

Shahabadi, N., & Hadidi, S. (2014). Molecular modeling and spectroscopic studies on the interaction of the chiral drug venlafaxine hydrochloride with bovine serum albumin. *Spectrochimica Acta - Part A: Molecular and Biomolecular Spectroscopy, 122*, 100–106. https://doi.org/10.1016/j.saa.2013.11.016.

Silva, C. E. L., Hudson, E. A., Agudelo, Á. J. P., da Silva, L. H. M., Pinto, M. S., do Carmo Hespanhol, M., ... Pires, A. C. S. (2018). β-Carotene and milk protein complexation: A thermodynamic approach and a photo stabilization study. *Food and Bioprocess Technology, 11*(3), 610–620. https://doi.org/10.1007/s11947-017-2028-7.

Silva, J. T.d. P., da Silva, A. C., Geiss, J. M. T., de Araújo, P. H. H., Becker, D., Bracht, L., &

Gonçalves, O. H. (2017). Analytical validation of an ultraviolet–visible procedure for determining lutein concentration and application to lutein-loaded nanoparticles. *Food Chemistry, 230*, 336–342. https://doi.org/10.1016/j.foodchem.2017.03.059.

Sobral, D., Bueno Costa, R. G., Machado, G. M., Jacinto de Paula, J. C., Martins Teodoro, V. A., Nunes, N. M., ... Pinto, M. S. (2016). Can lutein replace annatto in the manufacture of Prato cheese? *LWT - Food Science and Technology, 68*. https://doi.org/10.1016/j.lwt.2015.12.051.

Suryawanshi, V. D., Walekar, L. S., Gore, A. H., Anbhule, P. V., & Kolekar, G. B. (2016). Spectroscopic analysis on the binding interaction of biologically active pyrimidine derivative with bovine serum albumin. *Journal of Pharmaceutical Analysis, 6*(1), 56–63. https://doi.org/10.1016/j.jpha.2015.07.001.

Tan, T. B., Yussof, N. S., Abas, F., Mirhosseini, H., Nehdi, I. A., & Tan, C. P. (2016). Forming a lutein nanodispersion via solvent displacement method: The effects of processing parameters and emulsifiers with different stabilizing mechanisms. *Food Chemistry, 194*, 416–423. https://doi.org/10.1016/j.foodchem.2015.08.045.

Wang, K., & Arnt, S. D. (2015). Effect of salts and pH on selected ketone fl avours binding to salt-extracted pea proteins: The role of non-covalent forces, 77, 1–9. doi:https://doi.org/10.1016/j.foodres.2015.03.017.

Yi, J., Fan, Y., Yokoyama, W., Zhang, Y., & Zhao, L. (2016). Characterization of milk proteins-lutein complexes and the impact on lutein chemical stability. *Food Chemistry, 200*, 91–97. https://doi.org/10.1016/j.foodchem.2016.01.035.